

# Chemical Abundances of Planetary Nebulae in M33<sup>★</sup>

L. Magrini<sup>1</sup>, M. Perinotto<sup>1</sup>, A. Mampaso<sup>2</sup>, R.L.M. Corradi<sup>3</sup>

<sup>1</sup> Dipartimento di Astronomia e Scienza dello Spazio, Università di Firenze, L.go  
E. Fermi 2, 50125 Firenze, Italy

<sup>2</sup> Instituto de Astrofísica de Canarias, c. Vía Láctea s/n, 38200, La Laguna,  
Tenerife, Canarias, Spain

<sup>3</sup> Isaac Newton Group of Telescopes, Apartado de Correos 321, 38700 Santa Cruz  
de La Palma, Canarias, Spain

Received date /Accepted date

**Abstract.** Using spectroscopic data presented in Magrini et al. (2003), we have analyzed with the photoionization code CLOUDY 94.00 (Ferland et al. 1998) 11 Planetary Nebulae belonging to the spiral galaxy M 33. Central star temperatures and nebular parameters have been determined. In particular the chemical abundances of He/H, O/H, N/H, Ar/H, and S/H have been measured and compared with values obtained via the Ionization Correction Factors (ICFs) method, when available. Chemical abundance relationships have been investigated; in particular, a correlation between N/H and N/O similar to the Galactic one (Henry 1990), and a feeble anti-correlation between O/H and N/O have been found. A gradient in O/H across the disc of M 33 is indicatively consistent with the one found from H II regions in this galaxy (Vílchez et al 1988). Further studies in the more external parts of M 33 are however needed to ascertain this point. The present result shows that oxygen and helium abundances (with lower accuracy also nitrogen, argon and sulphur) can be actually estimated from the brightest PNe of a galaxy, even if the electron temperature cannot be measured. We also found that the oxygen abundance is quite independent of the absolute magnitude of the PN and consequently the brightest PNe are representative of the whole PN population. This represents an important tool to measure the metallicity of galaxies at the time of the formation of PNe progenitors.

**Key words.** Planetary nebulae:individual: M33 – Galaxies:individual: M33 – Galaxies: Abundances

## 1. Introduction

Chemical abundances in extragalactic Planetary Nebulae (PNe) have been derived so far only in a small number of galaxies. Inside the Local Group they are: the irregular galaxies LMC, SMC (cf. Leisy et al. 2000; Jacoby & De Marco 2002), and NGC 6822 (Richer & McCall 1995), the dwarf spheroidal and spheroidal galaxies Fornax (Maran et al. 1984), Sagittarius (cf. Walsh et al. 1997), NGC 185, and NGC 205 (Richer & McCall 1995), the elliptical galaxy M 32 (Stasinska et al. 1998) and finally the two spiral galaxies M 31 and M 33 that have been studied by Jacoby & Ciardullo (1999, hereafter JC99) and Magrini et al. (2003, hereafter M03), respectively. There is a substantial lack of information about chemical abundances of PNe in dwarf irregular galaxies of the Local Group (e.g. Sextans B, Sextans A, Leo A, IC 10), where no PN has been investigated so far. Outside the LG, only PNe in the giant elliptical galaxy NGC 5128 (Centaurus A) at the distance of 3.5 Mpc were analyzed by Walsh et al. (1999).

In most of the previous cases, with the exception of NGC 5128, the abundances have been obtained by direct determination of the  $T_e$ , derived from the [O III]  $\lambda\lambda$  4363/5007 Å or, in the worst cases when the  $\lambda$  4363 Å is not measured, using its upper limit, thus obtaining lower limits for the [O III] ionic abundance and then for the total O abundance, which was calculated from the ICFs (Ionization Correction Factors) procedure (cf. e.g. Kingsburgh & Barlow 1994, hereafter KB94).

In M 31, in addition to the ICFs method, JC99 have modeled the observed PNe using the photoionization code CLOUDY 90 (Ferland et al. 1998) with simplified assumptions: blackbody central stars and spherical nebulae with constant density. They have derived abundances and central star parameters for 15 PNe of M 31. In eight cases they could compare the results from the nebular models built with CLOUDY with abundances based on the ICFs method. They found good agreement between abundances derived with these two different methods. From this comparison, CLOUDY resulted to be a useful tool to measure chemical abundances, particularly when direct electron temperature measurements are not available.

M03 studied 48 emission line objects in M 33 spectroscopically, and recognized, via diagnostic diagrams, 26 of them to be *bona fide* PNe. They presented the observed fluxes for 42 of the 48 objects, deriving chemical abundances with the ICFs method for the three brightest PNe.

In the present paper, we re-analyze with CLOUDY 94.00 (Ferland et al. 1998) 11 of the 26 PNe presented by M03 using the available spectroscopic data. The three PNe

---

*Send offprint requests to:* L. Magrini

e-mail: laura@arcetri.astro.it

\* Based on observations obtained at the 4.2m WHT telescope operated on the island of La Palma by the Isaac Newton Group in the Spanish Observatorio del Roque de Los Muchachos of the Instituto de Astrofísica de Canarias.

already studied with ICFs by M03 are also included, in an effort to clarify their observed low N/O.

In Section 2 we summarize the observations and data reduction. In Section 3 the derivation of nebular and stellar properties is illustrated. In Section 4 we discuss the derived quantities and correlations among them. Summary and Conclusions are in Section 5.

## 2. Observations and data reduction

The observations were taken at the 4.2 WHT telescope (La Palma, Spain) in October, 2001 with AF2/WYFFOS, with a setting producing a dispersion of  $3.0 \text{ \AA}$  per pixel in the spectral range  $4300 \text{ \AA}$  to  $7380 \text{ \AA}$ . A detailed description of spectroscopic data and of the reduction procedure are in M03.

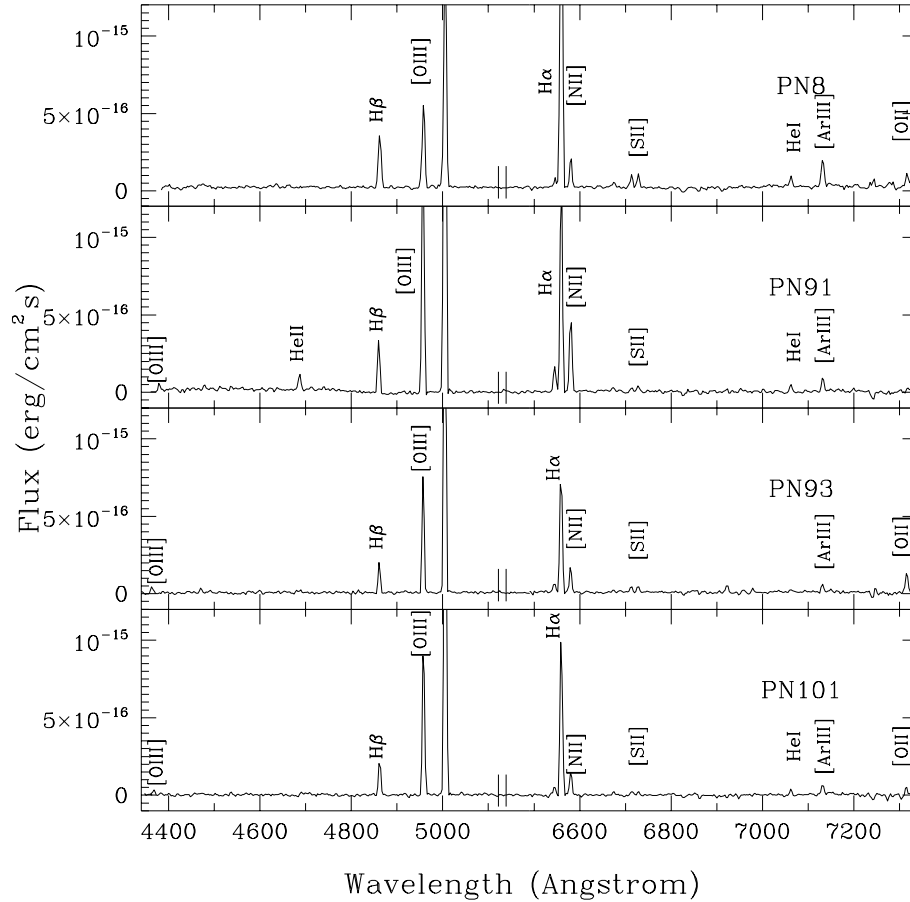


**Fig. 1.** Characteristic spectra of PNe in M 33 obtained by M03 with an exposure time of 8.7 hrs with the WHT.

### 3. The modelling procedure

Using a photoionization model such as CLOUDY, it is possible to overcome the lack of direct information on the electron temperature in a PN, due to the faintness of the relevant forbidden lines: the [O III]  $\lambda 4363$  and the [N II]  $\lambda 5755$  emission lines, which are hard to detect in extragalactic PNe. On the other hand, the use of CLOUDY requires as input the energy distribution of the ionizing radiation of the central star, its luminosity and the nebular geometry. The distance to the object must then be known. In our case the distance is available adopting for all PNe in M 33 the distance of the galaxy, equal to  $840 \pm 90$  kpc (Magrini et al. 2000, hereafter M00). As with the energy distribution of central stars, the usual simplification is to assume them to behave as blackbodies (BB), while for a better accuracy stellar atmosphere models are needed (cf. Morisset 2004). In this respect, an illustrative test was carried out by Howard et al. (1997). They tested the effects on derived abundances and central star temperatures of a variety of model atmospheres and blackbodies in a set of Galactic halo PNe. They found that nebular line strengths are relatively insensitive to atmospheric model details and that blackbody spectra are by and large suitable to represent the central star continua. On the other hand Armsdorfer et al. (2002) checked in the particular case of the spatially resolved round Galactic PN NGC 2438, the effects of modelling a PN central star with a blackbody instead than with a model atmosphere. They found that the BB assumption leads to underestimating the [O III]  $\lambda 5007$  line and to overestimating the He II  $\lambda 4686$  line strength. Therefore the assumption of BB central stars might introduce uncertainties in the determination of chemical abundances. We will also check in the next sections in a specific case the BB assumption vs. the use of a model atmosphere. We will see that differences in resulting abundances are quite small.

The aim of our procedure is to match the intensity of the observed emission lines with that predicted by CLOUDY. The spirit of our procedure is similar to the one adopted by JC99 to determine the chemical abundances of PNe in M 31. In the following we briefly describe how our analysis works.

CLOUDY needs the following input parameters: the central star energy distribution and luminosity, the nebular geometry, the electron density, and the chemical abundances. Because of the lack of information in our objects on the morphology and on the density distribution, we set the geometry to be spherical and the density to a constant value, although we will explore the effect of a  $r^{-2}$  density distribution in some PNe. The central star energy distribution was set to that of a BB. For the three PNe (PN91, 93, 101) with the best S/N spectra and with chemical abundances derived also with the ICFs method (M03), we will compare nebular abundances from the blackbody central star with those from the model atmospheres by Rauch (2003) (see Table2).

The first run is done setting the input parameters as follows. The BB temperature is derived using the Ambartsumian's method (Ambartsumian 1932), i.e. using the  $\text{He II}(4686)/\text{H I}(4861)$  line flux ratio, or the  $([\text{O III}](4959)+[\text{O III}](5007))/\text{He II}(4686))$  lines ratio method (Gurzadyan 1988) for medium and high excitation objects, respectively. The medium and high excitation is recognized from the observed line ratio  $\text{He II}(4686)/\text{H I}(4861)$ . Following Gurzadyan (1996) we call high excitation PNe those with  $\text{He II}(4686)/\text{H I}(4861) > 0.15$ .<sup>1</sup>

The central star luminosity is set to reproduce the observed absolute flux of the  $[\text{O III}] \lambda 5007$  nebular line, measured by Magrini et al. (2000) via aperture photometry and reddening corrected with  $E(B-V)=0.07$  (van den Bergh (2000)). We made an effort to correct each  $\lambda 5007 \text{ \AA}$   $[\text{O III}]$  flux with the individual reddening coming from the Balmer decrement. We saw that in some cases the corrected luminosity was substantially above the cutoff of the  $[\text{O III}]$  luminosity function. Thus we conclude that the de-reddening values from the Balmer decrement suffer from calibration issues. In these cases, while the line fluxes can be considered to be correct,  $c\beta$  is not appropriate to correct the photometric fluxes. We have then preferred to correct the photometric fluxes using the average extinction towards M 33.

We varied the external radius from  $10^{16} \text{ cm}$  ( $0.0032 \text{ pc}$ ) to  $10^{18} \text{ cm}$  ( $0.32 \text{ pc}$ ). This range corresponds to a reasonable interval of sizes of Galactic PNe. The electron density is evaluated from the  $[\text{S II}] \lambda\lambda 6717/6731$  line ratio. We have assumed the average non-Type I galactic PNe abundances from KB94 as initial chemical abundances and dust grains, with composition and size considered to be typical of Galactic PNe dust (cf. Ferland 1998). The addition of dust in the model does not vary substantially the derived chemical abundances.

Further iterations make the following adjustments. First the BB  $T_\star$  is altered to match the  $\text{He I}/\text{He II}$  line ratio. When the  $\text{He II} \lambda 4686$  line was too weak to be measured, we determined its upper limit so as to derive an upper limit to the central star temperature. These cases correspond to  $T_\star$  marked with b in Table 1, while directly measured stellar temperatures are marked with a. In the few cases, where the  $[\text{O II}] \lambda 7325$  doublet was measured, the nebular radius was varied to match the observed ratio of the nebular lines  $[\text{O III}] \lambda 5007$  and  $[\text{O II}] \lambda 7325$  (cases marked with c in Table 1) (cf. Che & Köppen 1983). In the other cases, models with different nebular radii were built. For these PNe, we found the smallest and the largest radius for which the model converged. Final quantities are the averages of quantities from models spanning over these nebular radius intervals (cases marked with d in Table 1).

---

<sup>1</sup> Gurzadyan (1988) indeed distinguishes between low and high excitation objects. We prefer to use the term 'medium' in place of low because when the  $\text{He II} \lambda 4686$  line is measured, the excitation cannot be really regarded as low. We think this specification is more appropriate to PNe where the line is not detectable.

Subsequently chemical abundances are varied in order to match the observed and predicted intensities within 5% for the lines brighter than  $H\beta$  and 20% for the other lines. The  $T_e$  derived from the model is compared with the observed one, when available, i.e. in the three PNe where the  $[O\ III]\ 4363\ \text{\AA}$  emission-line was measurable. In these PNe, the abundances of C and O (the most important coolants) were slightly modified to match the observed  $T_e$ . The optical depth of the nebula is derived from the hydrogen ionization structure predicted by the CLOUDY model. The PNe are optically thick, while a few with lower density (PN28, PN96, PN125) resulted to be optically thin.

Generally, we need from 10 to 30 iterations to reach convergence, i.e. to reproduce within 5-20% the observed line spectrum. Well determined quantities are the luminosity of the central star, because distance and absolute  $[O\ III]\ 5007\ \text{\AA}$  flux are both well known, and the temperature of the central star (when both He I and He II lines are measured). The determination of the nebular radius is instead weaker, because the measurement of  $\lambda\ 7325\ \text{\AA}\ [O\ II]$  doublet is affected by large observational errors. In two PNe where the  $[O\ II]\ \lambda 7325$  doublet was measured (PN 91, 93) we introduced the dependence on  $r^{-2}$  in the density to find better agreement between observed and predicted  $[O\ III]/[O\ II]$  ratio. In fact the ratio  $[O\ III]/[O\ II]$  is not only sensitive to the size of the nebula, but it depends also on several other parameters, mainly on the density distribution (cf. Che & Köppen 1983). When the central star temperature is derived from the upper limit of the He II  $\lambda 4686$  line, only upper limit to the helium and other metal abundances can be derived.

The derived central star temperatures and nebular quantities are shown in Table 1. We recall that the  $T_\star$  derived from the upper limit of the He II  $\lambda 4686$  are marked with b, whereas the directly measured  $T_\star$  are marked with a. Derived nebular radii are marked with c, and upper limit nebular radii with d.

In Table 2 chemical abundances for three PNe computed using ICFs (M03) are compared with current CLOUDY results. Note that for Ar/H the ionization correction factors are larger than one because only the  $[Ar\ III]\ \lambda 7135$  line is detected.

### 3.1. Tests of the procedure

We have tested the accuracy of the method by applying it to seven bright Galactic PNe (M1-8, M3-1, M3-5, NGC2867, NGC3195, NGC7009, NGC5852), using only the emission lines present in our extragalactic PN spectra, and comparing our results with the chemical abundances obtained with the ICFs method by KB94. PNe with central star BB temperatures spanning in a large range (from approximately 60,000 to 190,000 K) have been analyzed. For these tests we have used the basic approximations of our model: BB central star and constant density. The results are shown in Figures 2 and 3. We found a good agreement in the helium abundance, with a r.m.s. difference of 0.015 dex (triangles in Fig.2). The typical r.m.s. differences of the two determinations, with CLOUDY and

with ICFs, of O/H is 0.15 dex, of Ar/H is approximately 0.1 dex and of N/H is  $\sim 0.3$  dex. In some cases these quantities are underestimated by our method whereas sometimes are overestimated. On the other hand S/H and N/H appear to be generally underestimated by CLOUDY, with a r.m.s. difference of 0.2 dex. A possible explanation for the systematic differences in S/H and N/H determination might be related to the fact that for these two elements only low ionization lines are observed. The considered PNe are medium and high excitation objects where these ions represent only a minor fraction of the total elemental abundance. Moreover the ionization potential of [S II] is lower than that of [N II], which might explain the larger discrepancy in S/H.

#### 4. Chemical Abundances

We have applied the procedure above described to 11 PNe of M 33. In four cases we could determine the temperature of the central star within 5,000 K using He I and He II lines. In the remaining cases we estimated an upper limit to the central star temperature using upper limits to the He II  $\lambda 4686$  flux. Considering the errors in the observed fluxes, the uncertainties in the model representation, and the quality in the fit obtained, we estimate typical errors are: in He/H of 0.05 dex (0.10 dex when  $T_\star$  is an upper limit), of 0.2 (0.3) dex in O/H, and of 0.3 (0.4) dex in Ar/H and S/H, and of 0.4 (0.5) dex in N/H. We note that S/H is generally under-estimated by the CLOUDY method in our test with Galactic PNe, and also N/H appears low compared to ICFs method for the highest values of N/H.

Chemical abundances, central star parameters, nebular radius and electron density are shown in Table 1. Chemical abundances previously obtained for the three PNe with the ICFs method (M03) are shown in Table 2 together with the new determinations, both with BB and model atmosphere (Rauch 2003). The four sets of determinations are consistent within the errors. Since the difference of the chemical abundances derived with CLOUDY using the two stellar ionizing sources are rather small, we used for the remaining PNe a BB central star. The use of a density dependent on  $r^{-2}$  with a BB central star produces better agreement between predicted and observed [O III]/[O II] ratio. With this model we obtain a higher N/H and a lower O/H, and consequently a higher N/O than with ICFs method.

S/H has been re-derived because of a numerical mistake in the previous work (M03). The discrepancy of S/H computed with ICFs and with CLOUDY (both BB and model atmosphere) is  $\sim -0.2$  dex, confirming the result mentioned above that CLOUDY tends to slightly underestimate S/H.

The comparison in the brightest PNe of M 33 of abundances derived with the ICFs and those from photoionization models, confirms the accuracy of the CLOUDY procedure in measuring helium, oxygen, nitrogen and argon abundances.

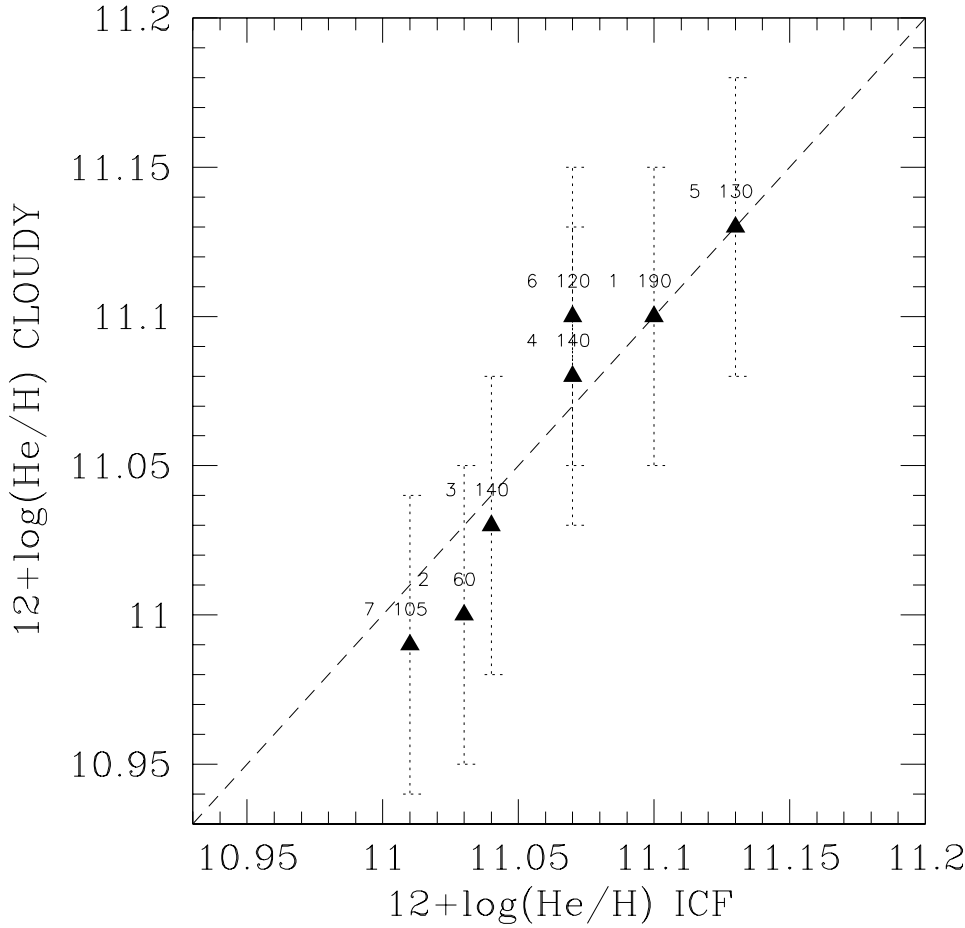


**Fig. 2.** Comparison of He/H abundance of a sample of Galactic PNe derived with ICFs method by KB94 with He/H computed using CLOUDY. Triangles represent He/H when  $T_{\star}$  has been derived in the present work. The id numbers refer to the Galactic PNe: 1–M1-8, 2–M3-1, 3–M3-5, 4–NGC2867, 5–NGC3195, 6–NGC7009, 7–NGC5852. The derived  $T_{\star}/1000$  is reported near to the corresponding measured He/H.

Stellar evolution theory predicts that He and N are enhanced in PNe by nucleosynthesis process, whereas elements heavier than N, like O, Ar, S do not vary significantly from the moment of the formation of their central stars (cf. Iben & Renzini 1983). In M 33, a comparison of our determinations of the chemical abundances of PNe (particularly for PNe whose  $T_{\star}$  could be measured, see Table 1) with those of H II regions (Vílchez et al 1988), especially for the best determined elements He/H and O/H (Table 1), confirms the reliability of the determinations. In fact, as expected, He/H (and also N/H, but remember the larger errors that affect this determination) is enhanced compared to H II regions while O/H is almost unchanged. This indicates that He and N have undergone nucleosynthesis enrichment in PNe progenitors, as theory predicts. Consequently N/O appears to be increased in the M 33 PNe compared with H II regions.

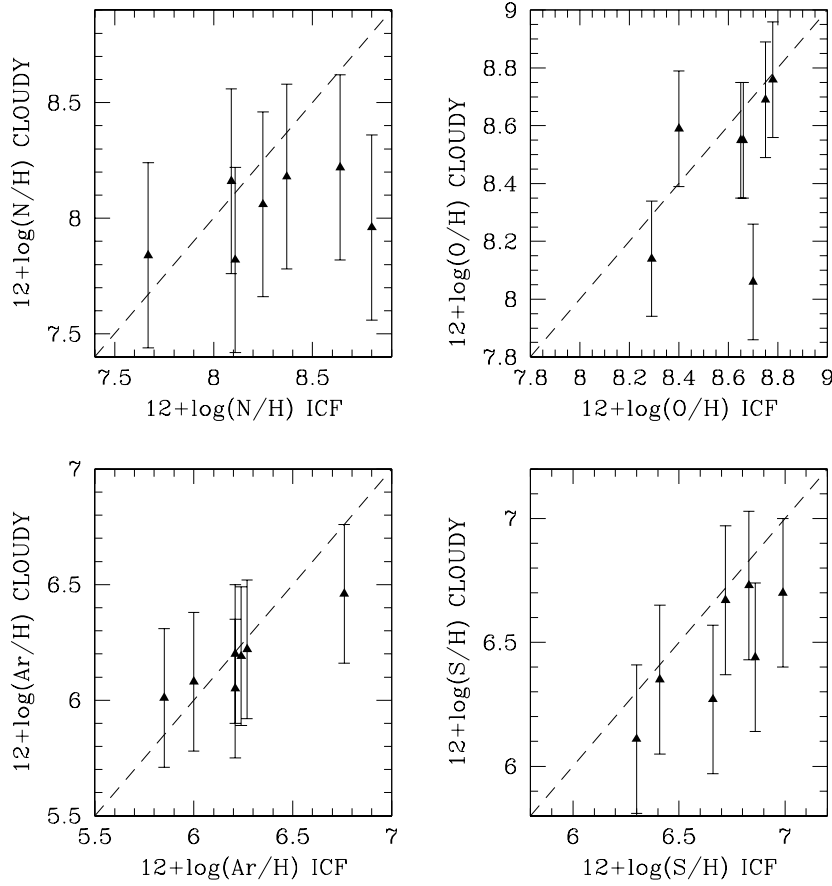


**Fig. 3.** Comparison of O/H, N/H, S/H, and Ar/H abundances of seven Galactic PNe derived with the ICFs method by KB94 with the same quantities computed using CLOUDY.

In Fig.4 we present the derived oxygen abundances as function of the galactocentric projected distance. We find a possible consistency with oxygen gradient across the disc of M 33 detected by Vílchez et al. (1988) for H II regions. A weighted least squares fit gives a  $\Delta \log(\text{O}/\text{H})/\Delta d = -0.14 \text{ dex kpc}^{-1}$ , assuming the distance of 840 kpc, to be compared with the overall gradient by Vílchez et al. (1988),  $\Delta \log(\text{O}/\text{H})/\Delta d = -0.10 \text{ dex kpc}^{-1}$ , considering the same distance. The Pearson correlation coefficient for our relationship is 0.6. ON the other hand our result is quite dependent on a single PN (n. 8). Therefore the study of more PNe at high galactocentric distances is needed to clarify this aspect.

#### 4.1. Relationship among chemical abundances

In Fig. 5a we show the relation between He/H and N/O. Chemical abundances are plotted with their errors. The area included inside the dashed lines is the locus of Galactic PNe, derived from Fig.3 in P04. Following the recent results by Exter et al. 2004 for both bulge

**Table 1.** Central star temperatures and nebular parameters. Chemical abundances are expressed in  $12+\log(X/H)$ . The line fluxes  $F_{H\alpha}$  and  $F_{[OIII]}$  are observed (M00). The adopted reddening correction is  $E(B-V)=0.07$  (van den Bergh (2000)).

| Id                               | d      | $F_{H\alpha}$                         | $F_{[OIII]}$ | $T_*$  | $\log(L_*/L_\odot)$ | $\log(r)$         | $\log(N_e)$      | He/H  | N/H  | O/H  | S/H  | Ar/H | N/O   |
|----------------------------------|--------|---------------------------------------|--------------|--------|---------------------|-------------------|------------------|-------|------|------|------|------|-------|
| M00                              | arcmin | $10^{-15} \text{ erg/cm}^2 \text{ s}$ |              | K/1000 |                     | cm                | $\text{cm}^{-3}$ |       |      |      |      |      |       |
| 8                                | 22     | 11.4                                  | 10.1         | 74 b   | 3.8                 | $16 < r < 18$ d   | 3.1              | 11.05 | 7.07 | 7.94 | 6.38 | 6.11 | -0.87 |
| 18                               | 13     | 3.0                                   | 14.2         | 100 b  | 4.1                 | $16 < r < 17.9$ d | 2.5              | 11.09 | 7.48 | 8.20 | 6.83 | 6.51 | -0.72 |
| 28                               | 12     | 2.9                                   | 13.9         | 142 a  | 3.7                 | $16 < r < 17.7$ d | 2.1              | 10.96 | 6.98 | 8.69 | 6.47 | 6.3  | -1.71 |
| 60                               | 13     | 1.4                                   | 3.4          | 160 a  | 3.1                 | 17 c              | 2.9              | 11.04 | 7.67 | 8.69 | 6.57 | 6.31 | -1.02 |
| 65                               | 8      | 10.1                                  | 5.6          | 128 b  | 3.2                 | $16 < r < 17.7$ d | 3.2              | 11.16 | 7.61 | 8.67 | 6.84 | 6.63 | -1.06 |
| 75                               | 11     | 4.4                                   | 12.5         | 96 b   | 3.5                 | $16 < r < 17$ d   | 3.9              | 11.14 | 8.03 | 8.49 | 6.81 | 6.41 | -0.46 |
| 91                               | 18     | 4.9                                   | 16.3         | 110 a  | 3.6                 | 17.0 c            | 3.6              | 11.31 | 8.07 | 8.48 | 6.60 | 6.18 | -0.41 |
| 93                               | 16     | 3.1                                   | 7.4          | 96 a   | 3.3                 | 17.2 c            | 3.7              | 10.93 | 7.75 | 8.47 | 6.66 | 6.09 | -0.72 |
| 96                               | 9      | 3.1                                   | 11.9         | 105 b  | 3.5                 | $16 < r < 17.9$ d | 1.9              | 11.06 | 7.43 | 8.76 | 6.44 | 6.33 | -1.33 |
| 101                              | 14     | 4.1                                   | 11.4         | 97 b   | 3.4                 | 17 c              | 2.5              | 11.07 | 7.33 | 8.72 | 6.18 | 6.27 | -1.56 |
| 125                              | 9      | 7.5                                   | 8.2          | 86 b   | 3.6                 | $16 < r < 17.9$ d | 2.2              | 10.93 | 7.53 | 8.31 | 6.66 | 6.14 | -0.78 |
| M 33 PNe all (1)                 |        |                                       |              |        |                     |                   |                  | 11.08 | 7.65 | 8.54 | 6.62 | 6.33 | -0.89 |
| M 33 PNe with $T_*$ measured (1) |        |                                       |              |        |                     |                   |                  | 11.09 | 7.78 | 8.61 | 6.60 | 6.28 | -0.83 |
| M 33 H II regions (2)            |        |                                       |              |        |                     |                   |                  | 10.92 | 7.34 | 8.55 | 6.95 | -    | -1.21 |
| Galactic PNe non-Type I (3)      |        |                                       |              |        |                     |                   |                  | 11.05 | 8.14 | 8.69 | 6.91 | 6.38 | -0.55 |
| Galactic PNe Type I (3)          |        |                                       |              |        |                     |                   |                  | 11.12 | 8.72 | 8.65 | 6.91 | 6.42 | +0.07 |
| Galactic H II regions (4)        |        |                                       |              |        |                     |                   |                  | 11.00 | 7.57 | 8.70 | 7.06 | 6.42 | -1.13 |
| LMC PNe non-Type I (5)           |        |                                       |              |        |                     |                   |                  | 10.96 | 7.46 | 8.35 | 6.81 | 5.95 | -0.90 |
| LMC PNe Type I (5)               |        |                                       |              |        |                     |                   |                  | 10.95 | 8.28 | 8.24 | 7.11 | 6.12 | +0.02 |
| LMC H II regions (6)             |        |                                       |              |        |                     |                   |                  | 10.97 | 6.97 | 8.38 | 6.67 | 6.92 | -1.41 |

(1) Present paper (average, by number, not by log);

(2) Vázquez et al. (1988);

(3) KB94;

(4) Dufour (1984)

(5) Leisy & Dennefeld (2004)

(6) Dennefeld (1989)

and disc Galactic PNe on N/O vs He/H, PNe with low N/O show also low He/H, but at  $N/O > 0.25$  the whole range of He/H is sampled. The existence of a relationship between He/H and N/O has been discussed thoroughly by KB94, who found no correlation, although a correlation in the Type I PNe alone might exist. This issue is difficult to assess because there are intrinsic problems in determining helium abundance such as the collisional corrections and the uncertain ionization fractions. The data of M 33 for N/O vs He/H suggest a behaviour similar to the galactic one, but further studies are in order to really ascertain that.

Fig. 5b shows O/H vs N/O. The existence of an anticorrelation between these quantities is particularly controversial in the literature. Our data indicate a weak anticorrelation, with a Pearson correlation coefficient of 0.5 (0.2 in case of a weighted anticorrelation). Moreover, it appears that, for  $12+\log(O/H) < 8.5$ , only high values of N/O are found, while there is a larger spread for higher O/H abundances. The existence of this effect has also been found in Galactic bipolar PNe (Perinotto & Corradi 1998),

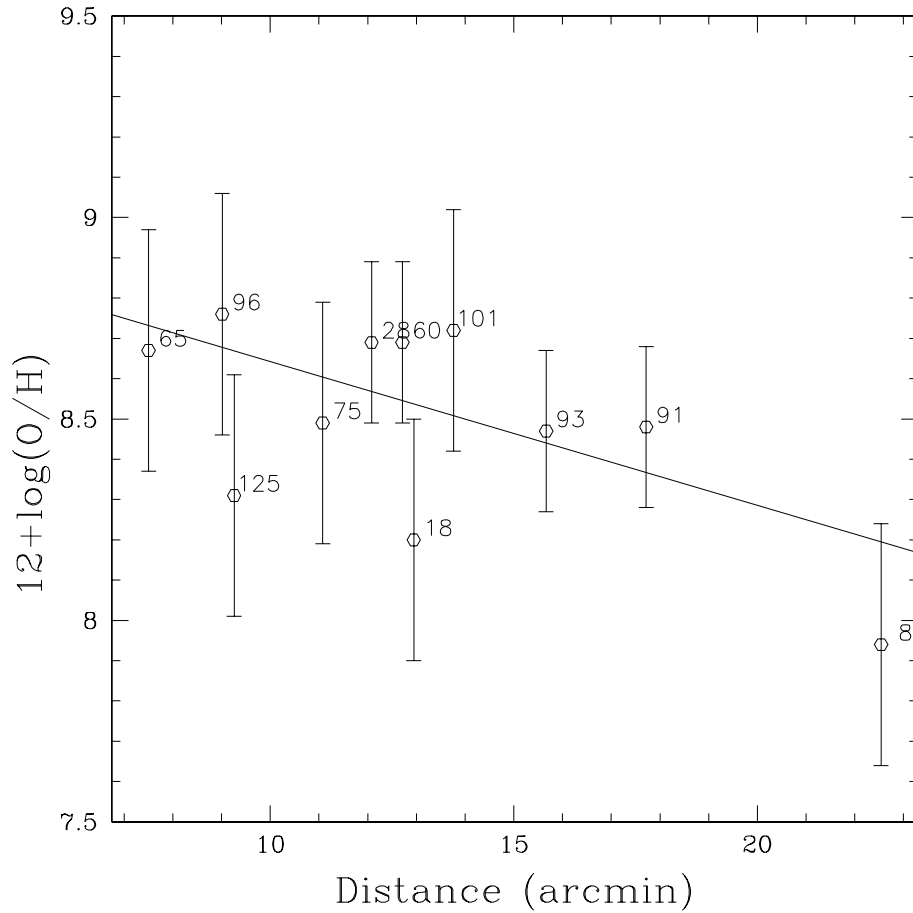


**Fig. 4.** The galactocentric trend of oxygen in M 33 from 11 PNe, recognized by their identification numbers in Table 1. The solid line is the galactocentric gradient found from H II regions by Vílchez et al. (1988) in the same galaxy.

in the Galactic bulge (Stasinska et al. 1998), in the SMC (Costa et al. 2000, Leisy & Dennefeld 2004), possibly in M31 (JC99) and the LMC (Leisy & Dennefeld 2004), although it is not apparent neither in the sample of Galactic PNe by KB94 (covering the range  $8.2 < 12 + \log(\text{O}/\text{H}) < 9.2$ ) nor in bulge and disc Galactic PNe by Exter et al. 2004 ( $8 < 12 + \log(\text{O}/\text{H}) < 9.2$ ).

In the cases where this transition to high N/O ratios for low oxygen abundances is well visible, it occurs at different O/H for different galaxies, and roughly at the average overall metallicity computed from other classes of objects like HII regions. This suggests that the explanation offered by Costa et al. 2000, i.e. the dredge-up increasing N/O in the AGB envelope is more efficient at low metallicities, might be not the main one, as the transition to high N/O ratios would then occur always at the same metallicity. Together with the fact that in the Galaxy the effect is better visible for high mass progenitors like bipolar PNe (Perinotto & Corradi 1998), the data would instead point to a high efficiency

**Table 2.** Comparison among CLOUDY both with blackbody central star and a constant density, with model atmosphere by Rauch (2003), and with BB and a density dependent on  $r^{-2}$  (two PNe) abundances determinations. The last row gives the ICFs abundances determinations (M03).

| Id  | Method                               | He/H  | N/H  | O/H  | S/H   | Ar/H |
|-----|--------------------------------------|-------|------|------|-------|------|
| 91  | CL <sub>BB</sub>                     | 11.31 | 7.86 | 8.61 | 6.42  | 6.26 |
|     | CL <sub>rauch</sub>                  | 11.20 | 8.01 | 8.64 | 6.52  | 6.25 |
|     | CL <sub>BB+dens-r<sup>-2</sup></sub> | 11.31 | 8.07 | 8.48 | 6.60  | 6.18 |
|     | ICF <sub>M03</sub>                   | 11.28 | 7.83 | 8.70 | 6.61† | 6.32 |
| 93  | CL <sub>BB</sub>                     | 11.00 | 7.53 | 8.69 | 6.46  | 6.17 |
|     | CL <sub>rauch</sub>                  | 10.92 | 7.55 | 8.60 | 6.44  | 6.13 |
|     | CL <sub>BB+dens-r<sup>-2</sup></sub> | 10.93 | 7.75 | 8.47 | 6.66  | 6.09 |
|     | ICF <sub>M03</sub>                   | 11.00 | 7.50 | 8.85 | 6.44† | 6.36 |
| 101 | CL <sub>BB</sub>                     | 11.07 | 7.33 | 8.76 | 6.18  | 6.27 |
|     | CL <sub>rauch</sub>                  | 11.14 | 7.34 | 8.70 | 6.13  | 6.22 |
|     | ICF <sub>M03</sub>                   | 11.15 | 7.21 | 8.72 | 6.32† | 6.45 |

†See text.

of the ON cycle in the most massive PN progenitors (Henry 1990), that would lower the O/H abundances while increasing N/O.

In Figs. 5c and 5d the relationship between N/O and N/H are presented. In Fig. 5c the dashed line represents the correlation found by Henry (1990) for the Galactic PNe. Our data, shown in Fig. 5c with their errors, show some scattering, but the Galactic relation between N/H and N/O appears to apply as well to M 33 PNe. The Pearson correlation coefficient is 0.7. JC99 suggested the meaning of this correlation: its slope is close to unity and thus the variations of N/O are mainly due to the variation of N/H (due to nucleosynthesis of N from progenitors of different mass), while oxygen abundance changes less during the life of PN central stars. In Fig. 5d, N/O vs. N/H is reported for Galactic PNe (P04), for PNe of the LMC (Leisy & Dennefeld 2004) and of M 33 (this paper). A similar trend is common to PNe of these three galaxies.

We come now to the number of Type I PNe in our sample. The Type I PNe, according to the definition of Peimbert & Torres-Peimbert (1983) are those with  $\log(\text{N/O}) \geq -0.3$  and high  $\text{He/H} \geq 0.125$ . A more stringent definition has been proposed by KB94,  $\log(\text{N/O}) > -0.1$ . On the other hand it has to be noted that the definition of Type I PNe should be a function of metallicity, because the amount of N that can be produced by hot bottom burning is dependent on the amount of C present and also because the O/H abundance depends on the metallicity of the galaxy. Thus a different criterion should be adopted for Type I PNe in a galaxy of different metallicity from our Galaxy. The N/O limit above

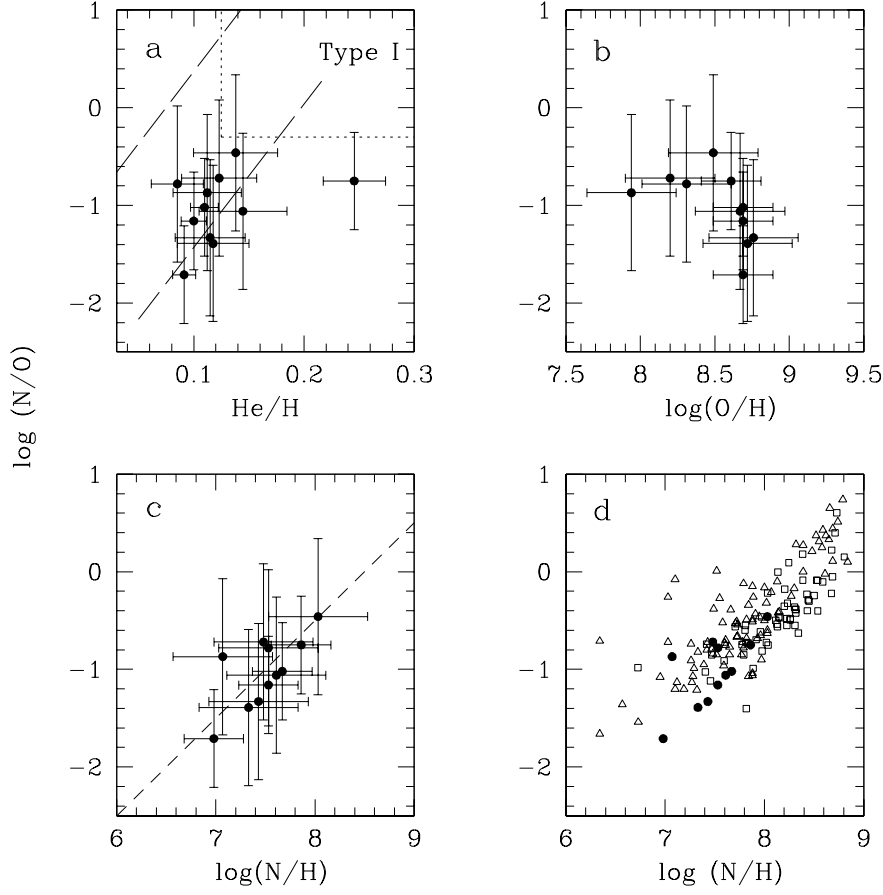


**Fig. 5.** Some relationships between chemical abundances. a) He/H vs. N/O. The area included inside the dashed lines is the main locus of Galactic PNe derived from Perinotto et al 2004, hereafter P04, Fig.3. The dotted lines show the limits of type I PNe area. b) O/H vs. N/O: an anti-correlation is shown as seen by JC99 in M 31; M 33 PNe (present paper) appear to reach lower N/O values than M 31 PNe. c) N/H vs. N/O. The dashed line shows the Galactic relation derived by Henry (1990) as shown by JC99. In spite of some dispersion, the Galactic relation between N/H and N/O appears to apply as well to M 33. d) N/H vs. N/O. Filled circles are PNe of M 33 (this work), triangles are PNe of LMC (Leisy et al. 2004) and squares are Galactic PNe (P04).

which a PN is a Type I, meaning that it has experienced hot bottom burning conversion of C to N, should be the C+N/O ratio from the H II regions. This is difficult to estimate since values for C are hard to obtain. Thus, since the metallicity of M 33 is not so different to that of our Galaxy, we still apply the Galactic criterion to discriminate Type I PNe. From Fig. 5a, we note a lack in M33 of type I PNe, using the Peimbert & Torres-Peimbert (1983) criterion. Moreover, we find no Type I PNe with the definition by KB94.

The average  $\log(N/O)$  of M 33 PNe is -0.89, see Fig. 5a. This value is lower than the Galactic non-Type I PNe (KB94) value (-0.55) and it is close to the non-Type I PNe value (-0.90; Leisy & Dennefeld 2004) of the LMC, which is a galaxy of similar metallicity (see van den Bergh 2000), whereas Galactic and LMC Type I PNe have a higher value (+0.07 and +0.02, respectively, see Table 1).

The number of Type I PNe might be connected to the metallicity of the host galaxy. In a deep survey for PNe of the SMC by Jacoby & De Marco (2002), they found an extremely large number of PNe where the  $[N\ II]$  lines are stronger than  $H\alpha$ . This might translate to a large Type I PN fraction. Comparing the fraction of Type I PNe also in the Galaxy and in the LMC, they determined that there might be a trend of more Type I PNe for lower metallicity galaxy. They explained this trend with the fact that more massive PN central stars, which are progenitors of Type I PNe, produce more dust and thus end up being systematically dimmer and consequently harder to detect. This would be more so on high metallicity galaxy since more dust should be produced. M 33, which has a metallicity intermediate between the Galaxy and the LMC, might be expected to have a similar number of Type I PNe (between  $\sim 17\%$  and  $\sim 20\%$  cf. Jacoby & De Marco (2002)).

An explanation for the smaller number of Type I PNe detected might be that Type I PNe, which are principally represented by bipolar morphological type and generally associated with younger and more massive progenitors (cf. Corradi & Schwarz 1995), are less luminous in the  $[O\ III]\ 5007\ \text{\AA}$  line than other morphological types of PNe (e.g. Magrini et al. 2004, see Figs. 1 & 2, from which one notes that the cutoff of bipolar PNLf is fainter  $\sim 1.5$  mag for LMC and  $\sim 2$  mag for the Galaxy than that of elliptical PNe). We remind the reader that the PNe presented in this paper have been discovered with a survey complete up to  $\sim 2$  mag fainter than the bright edge of the luminosity function (Magrini et al. 2000). If we consider that the results of luminosity functions of PNe with different morphology presented by Magrini et al. 2004, especially in the case of the Galaxy which has a similar morphology (M 33 is Sc III and the Galaxy is S(B)bc I-II, cf. van den Bergh 2000), apply to M 33 as well, this means that a number of bipolar Type I PNe could have been lost because of the incompleteness of the survey; i.e. one should expose more in  $[O\ III]$  to detect Type I PNe.

#### 4.2. Oxygen abundance and $[O\ III]$ luminosity

The determination of chemical abundances in an external galaxy rests on its brightest objects. We have examined the  $O/H$  vs  $[O\ III]$  luminosity in the M 33 sample, in the LMC, and in the Galaxy to test for possible biases in measuring  $O/H$  from the brightest PNe (see Fig.6). The sample of Milky Way PNe consists of objects in common between PNe whose chemical abundances have been re-determined by P04 and PNe whose distances

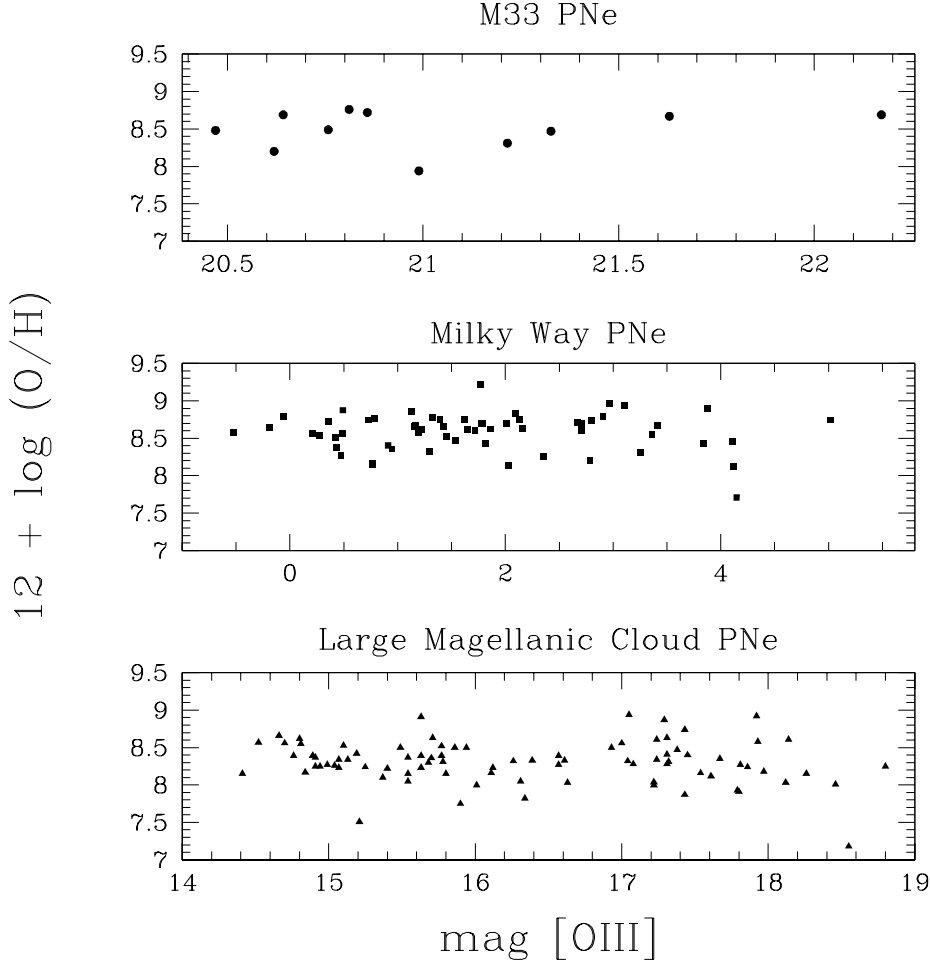


**Fig. 6.** [O III] luminosity vs O/H for M 33 PNe (upper panel), MW PNe (central panel) and LMC PNe (lower panel).

have been recently obtained by Phillips (2002), whereas the LMC sample consists of PNe with chemical abundances and relative fluxes from the work of Leisy & Dennefeld (2004), and the absolute fluxes from Jacoby et al. (1990).

One could expect that there would be a correlation between the oxygen abundance and the [O III] 5007 Å luminosity. However no trend of O/H vs [O III] luminosity is seen in the three galaxies, as already noted for M 31 by JC99. There might be various reasons for that. The basic point is that oxygen is one of the most important coolants of the nebula so that a high O concentration lowers the nebular temperature and consequently the flux coming from the [O III] 5007 Å line. There is therefore a feedback effect between a higher O/H concentration and a consequently lower  $T_e$  which produce the mentioned lack of trend of O/H vs. [O III] luminosity. It means that O/H derived from the brightest PNe (as from any PN) is representative of the total PNe population. This is particularly useful when deriving chemical abundances from PNe belonging to external galaxies, where only the brighter tip of their luminosity function is observed.

## 5. Summary and Conclusions

Using the CLOUDY photoionization code, we have derived nebular parameters and some stellar effective temperatures for 11 PNe belonging to the spiral galaxy M 33, and measured their He/H, O/H, N/H, Ar/H and S/H abundances. The data are consistent with the O/H gradient from H II regions by Vílchez et al. (1988), but abundances in PNe farther from the centre of M 33 than the sample studied here are needed to ascertain a clear metallicity gradient from PNe in M 33. A trend of N/O to N/H similar to the Galactic ones has been noted. We did not find PNe with the very high N/H and N/O values that are typical of galactic Type I PNe. A possible explanation is that the incompleteness of the survey for M33 PNe (M00) caused the loss of Type I PNe ( $N/O > -0.3$ ), which are generally faint in the [O III] 5007 Å emission line. Finally we found that the [O III] luminosity is clearly independent of the oxygen abundance. Therefore it is possible to use every PN, and particularly the brightest PNe, in external galaxies as representative of the whole PN population.

*Acknowledgements.* We especially thank Dr. Roberto Baglioni for his precious help in writing the Perl procedure. We are extremely grateful to an anonymous referee for comments and useful suggestions that improved significantly the paper.

## References

- Armsdorfer B., Kimeswenger S., & Rauch T., 2002, RMxAC, 12, 180 I
- Ambartsumian V. A., 1932, Poulkovo Obs. Circ 4, 8
- Che A. & Köppen J. 1983, A&A, 118, 107
- Corradi, R. L. M. & Schwarz, H., 1995, A&A, 293, 871
- Costa, R. D. D., de Freitas Pacheco, J. A., & Idiart T. P., 2000, A&AS 145, 467
- Dennefeld, M., 1989, in *Recent Developments of Magellanic Cloud Research*, eds. K.S. de Boer, F. Spite, G. Stasinska, Publ. Observatoire de Paris, Meudon, 107
- Dufour, R. J. 1984, In *IAU Symposium 108, Structure and evolution of the Magellanic Clouds* ed D. Reidel (Dordrecht:Reidel), 353
- Exter K. M., Barlow M. J., & Walton N. A., 2004, MNRAS, 349, 1291
- Ferland G. J., Korista K. T., Verner D. A., Ferguson J. W., Kingdon J. B., Verner E. M., 1998, PASP, 110, 761
- Gurzadyan G. A., 1988, ApSS, 149, 343
- Gurzadyan G. A., 1997, “The Physics and Dynamics of Planetary Nebulae” (Berlin: Springer), p. 112
- Henry R. B. C., 1990, ApJ, 356, 229
- Howard J. W., Henry R. B. C., & McCartney S., 1997, MNRAS, 284, 465
- Iben I. Jr. & Renzini A., 1983, ARA&A, 21, 271
- Jacoby G. H. & Ciardullo R., 1999, ApJ, 515, 169 (JC99)
- Jacoby G. H. & De Marco O., 2002, AJ, 123, 269
- Jacoby, G. H., Walker, A. R. & Ciardullo, R., 1990, ApJ, 365, 471

- Kingsburgh R. L. & Barlow M. J., 1994, MNRAS 271, 257
- Leisy P. & Dennefeld, M., 2004, in preparation
- Leisy P., Dennefeld M. & Francois, P., 2000, in Proceeding of Ionized Gaseous Nebulae. Mexico City November 21-24, 2000, p. 32
- Magrini L., Corradi R. L. M. & Mampaso A., Perinotto M., 2000, A&A, 355, 713 (M00)
- Magrini L., Perinotto M., Corradi R. L. M. & Mampaso A., 2003, A&A, 400, 511 (M03)
- Magrini L., Corradi R. L. M., Leisy, P. et al., 2004, in “Asymmetric Planetary Nebulae III”, ASP conf. series, in press
- Maran S. P., Gull T. R., Stecher T. P., Aller L. V. H. & Keyes C. D., 1984, ApJ, 280, 615
- Morisset, C., 2004, AJ, 601, 858
- Rauch, T., 2003, A&A 403, 709
- Richer M.G. & McCall M., 1995, ApJ, 445, 642
- Peimbert M. & Torres-Peimbert S., 1983, in IAU Symp. 103, Planetary Nebulae, ed. D.R. Flower (Dordrecht:Reidel), p. 233
- Perinotto M. & Corradi R. L. M., 1998, A&A, 332, 721
- Perinotto M., Morbidelli L., & Scatarzi A., 2004, MNRAS, in press (P04)
- Phillips, J. P., 2002, ApJS, 139, 199
- Stasinska G., Richer M.G. & Mc Call M.L., 1998, A&A, 336, 667
- van den Bergh S. 2000 in *The Galaxies of the Local Group*, Cambridge University Press
- Vílchez J.M., Pagel B.E.J., Diaz A.I., Terlevich E., Edmunds M.G. 1988, MNRAS 235, 633
- Walsh J. R., Dudziak G., Minniti D., & Zijlstra A. A., 1997, ApJ, 487, 651
- Walsh J. R., Walton N. A., Jacoby G. H. & Peletier R. F., 1999, A&A, 346, 753